Vol 16 No 10, October 2007
1009-1963/2007/16(10)/2918-06
Chinese Physics
© 2007 Chin. Phys. Soc.
and IOP Publishing Ltd

Neutralization process of Xe^{q+} ion grazing on Al(111) surface*

Hu Bi-Tao(胡碧涛)†, Zhang Hong-Jun(张宏俊), Zhang Jian(张 健), Song Yu-Shou(宋玉收), Wang Li-Li(王丽丽), Chen Chun-Hua(陈春花), and Gu Jian-Gan(顾建刚)

School of Nuclear Science and Technology, Lanzhou University, Lanzhou 730000, *China*

(Received 20 December 2006; revised manuscript received 2 February 2007)

A code has been developed to simulate the neutralization and grazing process of slow highly charged ion Xe^{q+} on Al(111) surface under the classical-over-the-barrier model. The image energy gain of Xe^{q+} ions are calculated and compared with experiment data. The simulation results of image energy gain are in good agreement with the experiment data. Meanwhile, in the present work, the reflection coefficient of incident Xe^{q+} on Al(111) surface as a function of the incidence angle, energy and charge state is also studied.

Keywords: slow highly charged ion, hollow atom, grazing incidence
PACC: 3000, 3120, 3400, 3440

1. Introduction

Because of low speed and high charge state of the slow highly charged ion (SHCI), the interaction between SHCI and a surface has special properties that ordinary ions do not have.[1] As the SHCI approaches a surface, it induces the collective response of the surface electrons, creating an image charge, which accelerates SHCI toward the surface. The neutralization of SHCIs starts above the surface and can be well described by the classical-over-the-barrier model (COBM) of ion–surface interactions.[2] When the SHCI reaches a critical distance above the surface, electrons from the surface are resonantly captured to the high-lying, quasi-stationary Rydberg state of SHCI.[3] This capture into the Rydberg states should continue until the SHCI becomes essentially neutral. This is the formation of hollow atom (HA). The initially present inner shell vacancies are still present. The HA will shrink rapidly by autoionization, but it will keep neutralization by ongoing resonant capture into high-lying Rydberg states. In addition, as the occupied Rydberg projectile states come into resonance with empty surface states, the electrons lying in the Rydberg projectile states can be recaptured back by the surface. The above resulting neutralization picture is a constantly shrinking electron cloud around the originally highly charged ion. Though the lifetime of HA is very short (typically about 100 fs), it can be studied by its electron emission, characteristic soft x-ray, trajectory, energy loss, and outgoing charge state after scattering from the surface.[4−6]

The present work simulates the process of the SHCI grazing incidence on Al(111) surface including neutralization process and scattering process based on Monte Carlo method. Atomic units are used unless otherwise stated.

2. Theory employed in simulation

2.1. Interatomic potential

The interaction between SHCI and crystal lattice atom of Al(111) separated by a distance R can be approximated by the screened Coulomb potential of the following form:

$$V(R) = (Z_1 Z_2/r) f(R/a_{\rm F}), \tag{1}$$

where $f(R/a_{\rm F})$ is the interatomic screening function with a length scale referred to screening length $a_{\rm F}$, which is determined by the following formula,[7]

$$f(R/a_{\rm F}) = \sum_i a_i \exp(-b_i R/a_{\rm F}), \tag{2}$$

*Project supported by the Research Fund for the Doctoral Program of Higher Education (Grant No 20030730004), the National Natural Science Foundation of China (Grant No 10374039) and the Natural Science Foundation of Gansu Province, China (Grant No ZS031-A25-001-Z).
†E-mail: hubt123@yahoo.com.cn

where $a_i = \{0.35, 0.55, 0.1, \ldots\}$, $b_i = \{0.3, 1.2, 6, \ldots\}$. For the interaction between SHCI and lattice atom of a solid surface, the following a_F is employed

$$a_F = 0.8854 \times ((Z_1 - q_1)^{2/3} + (Z_2 - q_2)^{2/3})^{1/2}, \quad (3)$$

where q_1 and q_2 are the charges bearing by the incident SHCI and target atom respectively.

When the projectile ions are far away from the surface of the crystal, interaction potential can be approximately described by[7]

$$U_p(R) = 2\pi n_s Z_1 Z_2 a_F \sum_i (a_i/b_i)\exp(-b_i R/a_F), \quad (4)$$

where n_s is the atom number per unit area of the crystal surface. The potential function depends strongly on the vertical distance R from the ion to the surface. As shown clearly in Fig.1, when the vertical distance to the solid surface R is small enough, the interaction potential between SHCI and Al atom has an obviously periodic structure as that of the crystal lattice. In order to save the computer time, only the interaction with the 75 crystal lattice atoms nearest to the projectile SHCI is taken into account in the simulation when R is small.

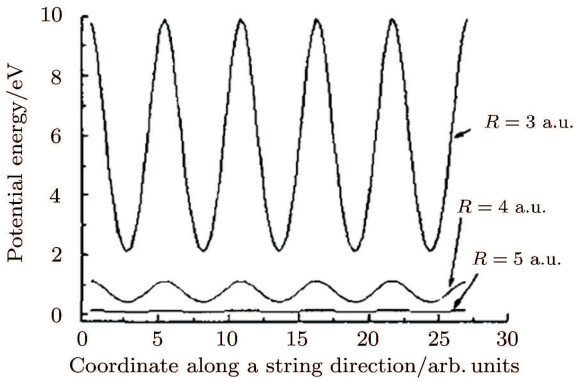


Fig.1. The interaction potential between incident ions and lattice surface along the direction of a string at different distances R.

2.2. Image potential

When an incident SHCI grazes against the metal surface, the quasi-free electrons of the surface will be rearranged to create an image charge. When the SHCI is slower than Bohr speed, it can be considered that the SHCI is static to interact with its image charge.[8] For a large R, the interaction potential between the ions and the image charge can be well described by

$$V(R) = -q/4R, \quad (5)$$

where q is the effective charge of the ions. The interaction potential can be corrected by the following equation when R becomes small[9]

$$V^I(R) = -q/4(z_0 + k_1 R + k_2 R^2), \quad (6)$$

where $z_0 = 1.025$, $k_1 = 0.9946$, $k_2 = 5.253 \times 10^{-5}$.

According to the COBM, the projectile ions start neutralization process with capturing the electrons when R reaches the critical distance as the ions approach the crystal lattice. The projectile charge state changes staircase-like (staircase model) as the projectile approaches the solid surface. The dependence of critical distance on charge state q of the projectile ions and work function of the solid target can be well described by the following:[3]

$$R_c = (1/(2W))(8q + 2)^{1/2}, \quad (7)$$

where W is the work function of the crystal. For Al(111), a more precise formula is used[9] in the simulation,

$$R_c = (1/(2W))(c_1 q + c_2)^{1/2}, \quad (8)$$

where $c_1 = 8.015$, $c_2 = 2.629$, $W = 4.28$ eV.

2.3. Energy loss

When the SHCIs graze against the surface of Al, they experience energy loss, which are induced from four sources: the charge exchange with the target above the surface; the excitation of the plasma above the crystal surface; the interaction with the quasi-free electron gas below the crystal surface; and the elastic collision with the crystal lattice atoms.

When the SHCI grazes against the crystal, charge exchange occurs, which can cause an energy loss. The energy loss in the single-charge exchange can be determined by the following equations:[10]

$$\Delta E_{cap} = (B_T - B_P) + (E_P m_P/(4m_T)) \times ((m_P+m)m_P - (B_T - B_P)/E_P - m/m_p)^2, \quad (9)$$

$$\Delta E_{loss} = 1/2 \times mv^2 + (m_P/(m_P + m)) \times (B_P + E_C) + E_P(m_p/4m_T) \times ((B_P + E_C)/E_P)^2, \quad (10)$$

where ΔE_{cap} and ΔE_{loss} denote the energy losses resulting from the electron capture and loss respectively; m_P, m_T and m denote respectively the masses of the projectile, target atom and electron; B_T and B_P the binding energies of the electrons with the target and the projectile cores respectively; E_p is the projectile

energy, v the laboratory-frame velocity of the projectile, and $E_{\rm C}$ the mean kinetic energy of electrons separated from the projectile.

When an ion approaches the metal surface, the electron density in the metal is rearranged to create image charge. The attractive interaction between projectile ion and its image charge causes the excitation of plasma and electron-hole on the crystal surface, which results in the energy loss.[11] These two kinds of energy losses can be described by the following two equations separately:

$$S_{\rm SRM}^{\rm pl} = 2\gamma_0/(\pi V^2\omega_{\rm s}^2)\int \omega^2 K_0(2b\omega/V){\rm d}\omega = \gamma_0 V/(8\omega_{\rm s}^2)l/(b^3), \quad (11)$$

$$S_{\rm SRM}^{\rm ph} = 3V\ln(0.983q_{\rm TF}b)/(2\pi q_{\rm TF}^4)1/(b^4), \quad (12)$$

where $\gamma_0 = 0.03$ a.u., $\omega_{\rm s}$ denotes the classic frequency of planar plasma, $q_{\rm TF}$ the Thomas-Fermi wave vector, V the velocity component parallel to the surface, and b the vertical distance to the surface.

When the projectile is close enough to reach the electron gas of the solid surface (< 6 a.u.), we assume that the projectile enters the electron gas in the bulk of the solid and adopt an empirical model based on the velocity-dependent electron-stripping criterion in which the ionization degree shows a remarkably good agreement with experimental values for heavy ions in solid.[12] When the projectile velocity is less than the Fermi velocity of the electron gas the local-field corrected (LFC) dielectric function can provide a more accurate description of the excitations of the surface electron gas by including the exchange-correlation interaction among the electrons. Based on the distribution of the electron gas above and below the metal surface, the position-dependent electronic stopping power can be expressed as[13,14]

$$S_{\rm e}(z_0) = 2k_{\rm F}^2 v/v_{\rm F}\int_0^1 k{\rm d}k(\tilde{\sigma}_n(k))^2 H(k,z_0'), \quad (13)$$

$$\tilde{\sigma}_n(k) = Z_1(q(z_0) + (2kk_{\rm F}\Lambda)^2)/(1+(2kk_{\rm F}\Lambda)^2), \quad (14)$$

$$H(k,z_0') = 2f_i(k)/(1+f_r(k))^2\exp(-4k_{\rm F}z_0'k), \quad (15)$$

where Z_0' and Z_0 denotes respectively the distances to the surface and first layer of lattice atoms, Λ is the screening length, $k_{\rm F}$ and $v_{\rm F}$ denote the Fermi wave number and Fermi velocity respectively, k is the wave vector of the incident ions, $q(z_0)$ the ionization degree of the ions at z_0, $f_i(k)$ and $f_r(k)$ are two integral functions well described in Refs.[13,14].

When the SHCIs interact with the crystal lattice atoms of Al(111), the momentum transfer from the projectiles to the lattice atoms takes place, which is called elastic energy loss or nuclear energy loss. For an estimate of the energy loss via binary elastic collisions, one finds that the elastic energy loss can be described by the following equation:[15]

$$\Delta E = (1-1/(1+(M_2/M_1)^2) \times (\cos\theta_1 + ((M_2/M_1)^2 - \sin^2\theta_1)^{1/2})^2)E_0, \quad (16)$$

where E_0 denotes the initial energy of the ions, M_1 and M_2 are the atomic masses of the projectile ion and target atom respectively, and θ_1 is the scattering angle of the ions.

3. Monte Carlo simulation

A code, STARF, is developed for the simulation, in which Xe^{q+} is selected as the incident SHCI, and the coordinate system is set as Fig.2.

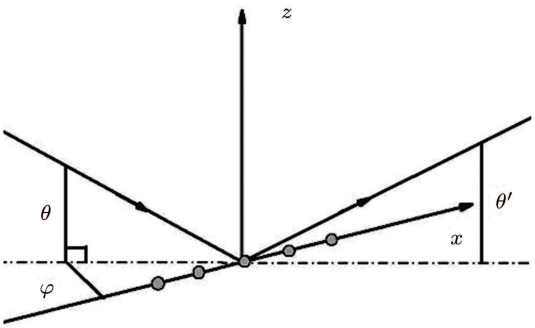


Fig.2. Coordinate system set up with the x axis along a string direction and the z axis perpendicular to the lattice surface. The top lattice layer is XOY surface; θ and ϕ are the incident and azimuth angles respectively.

In the present simulation, when $R > 5$ a.u., the potential is given by Eq.(4); when $R \leq 5$ a.u., the interaction is approximated by summing over all the interactions with the 75 crystal lattice atoms nearest to the projectile. The projectile ion approaches the surface step by step. In each step, the force between the projectile and the 75 lattice atoms are treated as a constant, by which the projectile experiences in the middle stage of the step. In order to save the computing time, let the step length be R-dependent and becomes shorter and shorter as R gets smaller.

The interaction of a multicharged ion with the surface is a true many-body problem. The charge transfer occurs mainly through resonant and Auger processes. A theoretical analysis of the neutralization dynamics above the surface has been presented

on the basis of the COBM[2,3] in which resonant multi-electron capture of conduction electrons, resonant loss into the unoccupied states of the conduction band, and the intra-atomic Auger de-excitation were considered and the transient formation of hallow atoms was described. In addition, in the close vicinity of the target surface, the outer shell electrons of the projectile ion can be peeled off by scattering with target surface electrons. In the present simulation we use the same approach in terms of coupled rate equations in which enter cross sections and rates for capture, loss, peeling off and de-excitation to simplify this fairly complex array of process as in Refs.[16, 17] and the references therein:

$$\begin{aligned} v_\perp(R)\frac{\mathrm{d}}{\mathrm{d}z}P_n(R) = {} & I_n^{\mathrm{c}}(R) - I_n^{\mathrm{l}}(R)P_n(R) \\ & - I_n^{\mathrm{p}}(R)P_n(R) \\ & + \frac{1}{2}\sum_{n'>n} A_{n,n'}P_{n'}^2(R) \\ & - P_n^2(R)\sum_{n'<n} A_{n',n}, \end{aligned} \tag{17}$$

where R is the projectile-surface distance, $v_\perp$ the projectile velocity in the direction normal to the target surface, P_n the electron population in the nth shell of the projectile, I_n^{c} the current of captured electrons, I_n^{l} the current of electron lost, $A_{nn'}$ the Auger rate of a projectile, and I_n^{p} the decay constant due to the peeling-off process.

4. Simulation results and discussion

4.1. Neutralization process

In the present work, the neutralization process of Xe^{54+} ions grazing against Al(111) is simulated. As shown in Fig.3, the neutralization process starts at R around 66 a.u. and as the projectile is getting closer to the solid surface, more and more electrons are captured to the high-lying Rydberg states leaving the inner states empty. Accompanying the neutralization process, the de-excitation is taking place. This is the reason why the electron population states move from the higher lying states to lower lying states when the projectile approaches the Al(111) surface. As shown in Fig.3, the projectile becomes neutral at R around 12 a.u..

Figure 4 shows the charge state q of Xe^{54+} ion as a function of R. The results of staircase model are shown in Fig.4, too. The horizontal dashed line is for the simulation and the vertical dashed one for the staircase model. As shown in Fig.4, because the states of the projectile have energy spread, the distance R at which the projectile captures the electrons from the surface has spread, thus R in the present simulation generally agrees well with R_{c} from the staircase model. When the projectile is too close to the solid surface ($R < 10$ a.u. as shown in Fig.4), the captured electrons in outer shell can be peeled off and the projectile charge state q can increase to 1–5.

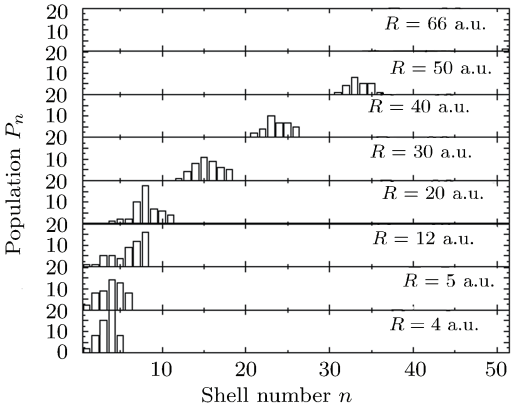


Fig.3. The dependence of electron population of different shells on distance R from the surface when the 100 keV Xe^{54+} ions grazes against the Al(111) surface at an incident angle of 1°.

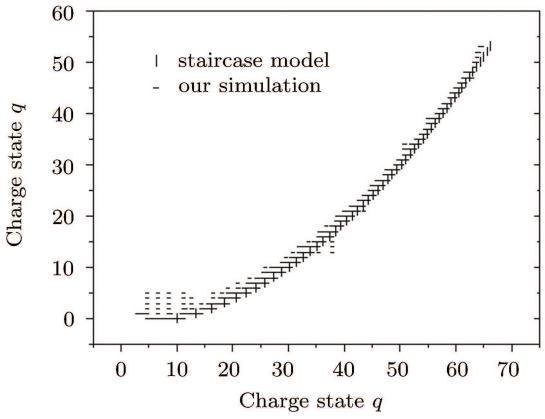


Fig.4. The dependence of the 100 keV Xe^{54+} ion's charge state q on distance from Al(111) surface when it's scattering on Al(111) surface.

In our simulation, the image energy gain as a function of charge state q of the projectile Xe is also simulated and the simulated results are shown in Fig.5. As shown in Fig.5, when $q < 35$, the simulation results are in good agreement with experimental data from Ref.[18] though they are a little higher than those of staircase model. When $q > 35$, the simulation results agree very well with the results of staircase model.

This is reasonable since the staircase model is a good approximation when the projectile charge state is high enough.

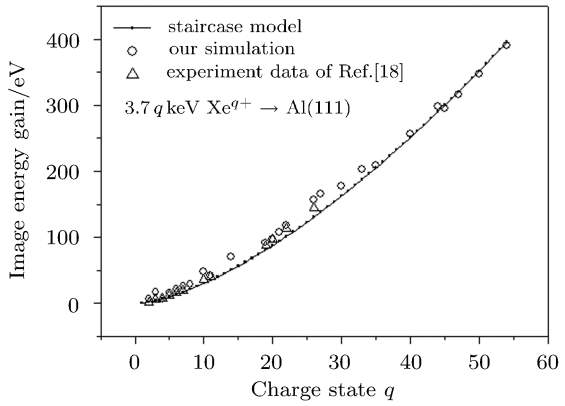


Fig.5. The image energy gain as a function of the charge state q of Xe ion when it is scattered on Al(111) surface at an energy of 3.7 q keV and incident angle of 1.5°.

4.2. Features of trajectories

Both the collective repulsive potential from the crystal lattice atoms and the attractive image potential will affect the trajectories. Since the image potential depends on the charge state of the projectile, the charge exchange process will play an important role on the trajectories. In the present work, we focus our attention on the surface channelling. When it happens, all the projectiles reach the same distance of closest approach and reflect symmetrically with respect to the crystal lattice atom string if the incoming and outgoing ions have the same charge state.

The reflection coefficient of the 3.7 q keV Xe^{q+} grazing against Al(111) surface at an incident angle 1.62° is simulated and compared with the results of Ref.[9]. The reflection coefficient as a function of the projectile charge state q is shown in Fig.6. As shown in Fig.6, when $q < 20$, the reflection coefficient is 100 percent. With increasing q, the kinetic energy component normal to the solid surface increases, and when $q > 20$, it becomes large enough to overcome the repulsive collective potential from the solid surface and the projectile starts to get into the crystal. From Fig.6, we can clearly see that our results agree with those of Ref.[9] reasonably well. The slight discrepancy at higher q between the present results and those of Ref.[9] is due to the fact that the screening length a_{F} is calculated differently from Ref.[9] by taking into account the influence of the projectile on the electron cloud of Al(111) lattice atom.

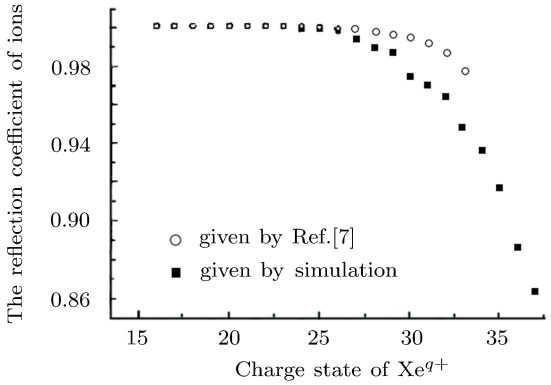


Fig.6. The dependence of the reflection coefficient on the charge state q for 3.7 q keV Xe^{q+} ions grazing against Al(111) at an incident angle $\theta = 1.62°$.

Meanwhile, the influence of charge state of the projectile ion on the trajectory is also studied. Assuming that the outgoing Xe atom is neutral, the incident angles θ (input data) and calculated exit angles θ' are both shown in Fig.7, in which the solid squares are the incident angles θ and open circles the exit angles θ'. The two-degree-shift between θ and θ' are due to energy gain of normal motion caused by the image charge interactions. So the present simulation clearly support the viewpoint that the data of the shift between θ and θ' allow one to reduce the image energy gain, and further the information on the total transient rates.

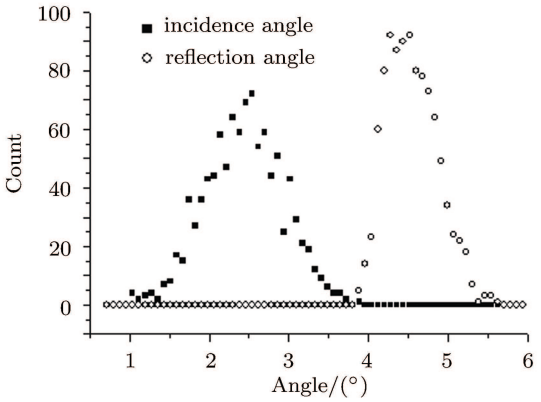


Fig.7. The distribution of incident and reflection angles for the 30 keV Xe^{30+} ions incident on Al(111) at an angle $\theta = 2.5°$.

To study this problem in detail, it is useful to separate the energies for motions normal and parallel to the surface plane

$$E_{//} = E_0 \cos^2 \theta, \tag{18}$$

$$E_{\perp} = E_0 \sin^2 \theta, \tag{19}$$

where E_0 and θ denote the incident kinetic energy and angle, respectively. From these two equations, we have

$$\mathrm{tg}^2\theta = E_\perp / E_{//}, \tag{20}$$

$$\Delta\theta = \Delta E_\perp \cos^2\theta/(2\sin\theta) \approx \Delta E_\perp/(2\theta), \tag{21}$$

As shown in Eq.(20), when the SCHI approaches the solid surface, the image potential energy gained is added to the energy of normal motion, which causes the increase of the real incident angle and consequently the exit angle under the surface channelling condition. This explains why θ' has two-degree shift relative to θ. Equation (21) shows that if the distribution of normal-motion-energy $\Delta E_\perp$ is kept unchanged, the increase of angle θ can cause the decrease of the angle distribution. Keeping this fact in mind, we can expect that the peak for θ' in Fig.8 is narrower than the peak for θ since θ' is larger than θ.

However, as shown in Fig.6, with increasing charge state of the projectile or incident angle, the effect of surface channelling becomes weak, which makes the exit angle θ' smeared. This is why we see in Fig.8 that with increasing incident angle, the distribution of exit angle becomes wider and wider.

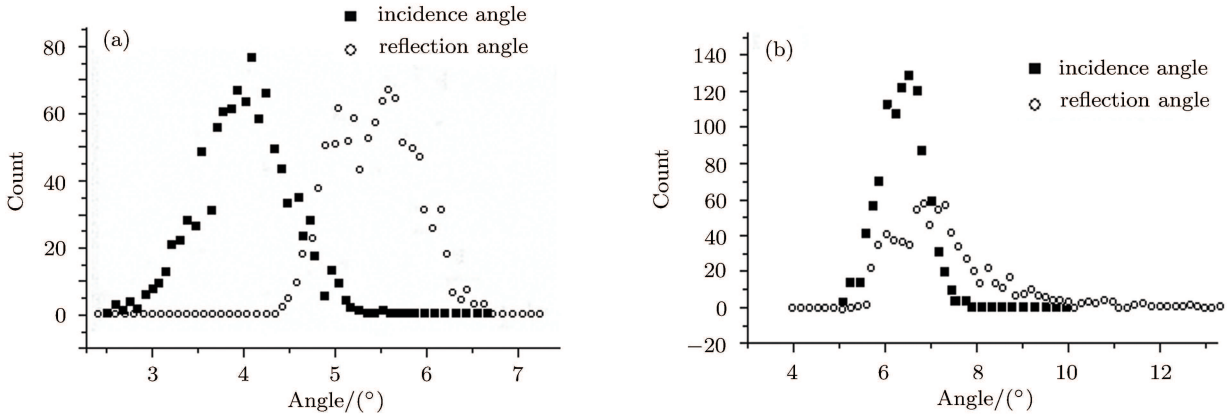


Fig.8. The distribution of incident angle θ and exit angle θ' when Xe^{q+} ($q = 30$) ions with initial kinetic energy $1.0q$ keV grazing against the Al(111) surface. (a) $\theta = 4.0°$, (b) $\theta = 6.0°$.

References

[1] Schenkel T, Hamza A V, Barnes A V, ?*et al*(补全) 1999 *Prog. Surf. Sci.* **61** 23

[2] Winter H 1999 *At Mol. Opt. Phys.* **32** R39

[3] Burgörfer J Lerner P and Fred W M 1991 *Phys. Rev.* A **44** 5674

[4] Winter H and Aumayr F 1999 *J. Phys.* B **32** R39

[5] Yang Z H, Song Z Y, Chen X M, Zhang X A, Zhang Y P, Zhao Y T, Cui Y, Zhang H Q, Xu X, Shao J X, Yu D Y and Cai X H 2006 *Acta Phys. Sin.* **55** 2221 (in Chinese)

[6] Yang Z H, Du S B, Zheng X T, Ren S T, Song Z Y, Su H and Wang Y D 2006 *Acta Phys. Sin.* **55** 2206 (in Chinese)

[7] Winter H 2002 *Physics Reports* **367** 387

[8] Ducrée J J, Casali F and Thumm U 1998 *Phys. Rev.* A **57** 338

[9] Yamamura Y and Fujii T 1999 *Nucl. Instr. Meth.* B **153** 242

[10] Bridwell L B, Hay H J, Pender L F, Sofield C J and Trac Y P B 1988 *Aust. J. Phys.* **41** 681

[11] Tökési K, Tong X M, Lemell C and Burgdörfer J 2005 *Phys. Rev.* A **72** 022901

[12] Ziegler J F Bieeisack J P and Littmark U 1985 *The stopping and Ranges of Ions in Matter* (Pergamon, Oxford) Vol. 1

[13] Song Y H, Wang Y N and Miskovic Z L 2001 *Phys. Rev.* A **63** 052902

[14] Wang Y N and Liu W K 1996 *Phys. Rev.* A **54** 636

[15] Mashkova E S and Makhanov V A 1985 *Medium-Energy Ion Reflection from Solids Modern Problems in Condensed Matter Sciences* (Amsterdam: North-Holland) Vol.11

[16] Wirtz L Reinhold C O Lemell C and Burgdörfer J 2003 *Phys. Rev.* A **67** 012903

[17] Yamamura Y, Nakagawa S T and Tawara H1995 *Nucl. Instr. Meth.* B **98** 400

[18] Winter H and Auth C 1993 *Phys. Rev. Lett.* **71** 1939